Tribology and Materials
Vol. 4, No. 2, 2025, pp. 78-89

ISSN 2812-9717
https://doi.org/10.46793/tribomat.2025.008

Achieving industrial-grade purity in recycled copper scrap: Pretreatment and fire refining approach

Omar CHOUKRI *, Mohsine EZ-ZINE, Souadi TAIBI

Mohammadia School of Engineers, Mohammed V University, Rabat, Morocco
*Corresponding author: o.choukri@emi.ac.ma

Keywords
recycled copper
pretreatment
fire refining
purity
impurities

History
Received: 20-03-2025
Revised: 25-04-2025
Accepted: 30-04-2025

Abstract

As global demand for copper continues to grow, recycling has become a critical component of sustainable resource management. In 2022, recycled copper constituted 32 % of the total global consumption of this metal, significantly reducing the pressure on natural resources. Recycling between 40 and 65 % of copper scrap could significantly reduce the demand for primary metals, especially in regions with high industrial growth. Many studies have focused on purifying secondary copper and its scrap under specific conditions with expensive equipment, limiting their application in industrial environments. This study proposes an economical process, accessible to small foundries, based on pretreatment and fire refining around the copper's melting temperature of 1080 °C. Tested on three types of copper scrap samples, this process yielded satisfactory results, with copper purity approaching 4N (99.99 %) and a 23 % reduction in impurities. Additionally, the final product demonstrated excellent performance, exhibiting electrical conductivity exceeding 86 % IACS (International Annealed Copper Standard) and nearing 90 % IACS. This quality makes it suitable for various industrial applications according to certain standards. Therefore, this process will contribute to promoting the circular economy by optimising the valorisation of copper scrap and reducing the environmental footprint of its processing.

1. Introduction

Recycling copper scrap offers significant economic and environmental advantages. Economically, it helps meet the growing global demand for copper because it can be recycled indefinitely without losing its physical, electrical and mechanical properties [1,2]. Moreover, producing copper from scrap requires only a quarter of the energy needed to extract it from ore and reduce greenhouse gas emissions [3,4]. For instance, the implementation of recycling as an effective strategy is anticipated to result in a substantial reduction in carbon emissions during processing activities. If the recycling rate exceeds 40 %, emissions should gradually fall to negligible levels by the end of the century. On the other hand, a more pronounced reduction towards zero will be achieved for recycling rates of between 60 and 80 % by 2080 [5,6].

Various standard techniques have long been employed in the copper recycling industry to discern and segregate scrap effectively. These include identification based on object recognition, colour, apparent density, magnetic attraction, stripping machine technology, mechanical crushing sorting technology, high-pressure water jet recovery technology, cryogenic technology, heat recovery technology, ultrasonic separation technology and chemical spot tests [7-10]. When properly applied by skilled sorters to mixtures of copper scrap, these techniques permit effective identification and segregation into specified categories [11,12].

Three smelting steps are employed to extract high-purity copper from copper scrap originating from post-consumer waste and other urban waste streams. The initial smelting stage is referred to as "reduce smelting", which yields black copper rich in

base metals. The second stage involves "converting", during which the black copper undergoes oxidation to produce raw copper and by-products. The raw copper can then be further processed in conventional anode furnaces to yield anode copper, which is subsequently electro-refined to produce cathode copper, nickel products and precious metals slime products [13,14].

Obtaining ultra-pure copper presents challenges due to the strong attraction of certain metallic and non-metallic impurities to copper, as well as high vapour pressure values and equilibrium segregation coefficients that are close to 1 for most impurity metals [15]. The presence of impurities significantly impacts its mechanical, electrical and physical properties [16]. Consequently, numerous researchers have endeavoured to achieve ultra-pure copper through various purification methods, e.g. applied voltage [17], zone melting [18], beam melting [19], induction vacuum furnace [20,21], electrolytic refining [22], oxidation impurities [23], vacuum melting and directional solidification [24] and zone refining [25], involving specialised equipment and specific conditions. Some studies [26,27] show that in pyrometallurgy, the highest level of copper purification that has been achieved is 5N (99.999 %), considering that the raw material was 4N (99.99 %) or 3N (99.9 %). In contrast, 6N (99.9999 %) purity has been achieved with advanced work in hydrometallurgy.

This paper presents the results of an experimental study conducted on copper scrap, taking advantage of the low impurity levels inherent in the scrap (particularly sulphur), undergoing fire refining with the integration of a simple pretreatment phase. The principal aim of this research was to ascertain the optimal temperature that maximises copper purity while concurrently minimising impurity levels through oxidation and volatilisation [28]. This significant advancement has been accomplished without specialised equipment or complex methodologies employed in previous studies. The proposed approach presents a cost-effective and accessible refining strategy, thereby facilitating the production of black copper for small-scale foundries engaged in the copper recycling industry.

2. Materials and methods

The experiments were conducted in an industrial environment, within a small foundry located in Morocco. These experiments focused on three specific samples averaging 250 g, selected from the scrap materials typically melted down by this foundry to produce semi-finished products. The first sample, classified as *Berry* according to the Institute of Scrap Recycling Industries (ISRI) [29], consisted exclusively of bare copper cables. The other two, classified as *Cliff* according to the ISRI, comprised a heterogeneous mixture of scrap. The Cliff samples primarily included winding wires, electrical wires, pieces of copper plates and tubes, copper shavings, connecting elements and parts from household appliances and cars.

First, the fire refinement was performed on the clean Berry sample (Fig. 1) to determine the values of copper and impurity concentrations in the baths at temperatures ranging from 1090 to 1180 °C with an increment of 10 °C. As it is used in telecommunications due to its high copper content, these values will serve as references for the rest of this study. Furthermore, due to the uniform wire configuration of this sample, its chemical composition, especially the impurity levels, was evaluated using a SPECTRO xSORT energy-dispersive X-ray fluorescence spectrometer (Table 1).

Similarly, fire refining of two Cliff copper scrap samples is carried out (Fig. 2) to determine the concentrations of copper and impurities in their baths at the mentioned temperatures. One of these Cliff samples (Fig. 3) underwent a pretreatment. This pretreatment included water washing in a rotary drum, air drying, heating in a Gold Tool GT-072F burnout furnace, with a power of 6 KW, at 300 °C for 15 min, followed by another water washing in a rotary drum and finally, air drying again (Fig. 4).

Figure 1. Berry sample

Figure 2. Untreated Cliff sample

Figure 3. Treated Cliff sample

Table 1. Impurities (wt. %) in a Berry sample (before melting)

Element	Al	Co	Ni	Pb	Se	Sn	Zn
wt. %	<0.082	<0.006	0.04	<0.019	0.02	<0.019	0.051

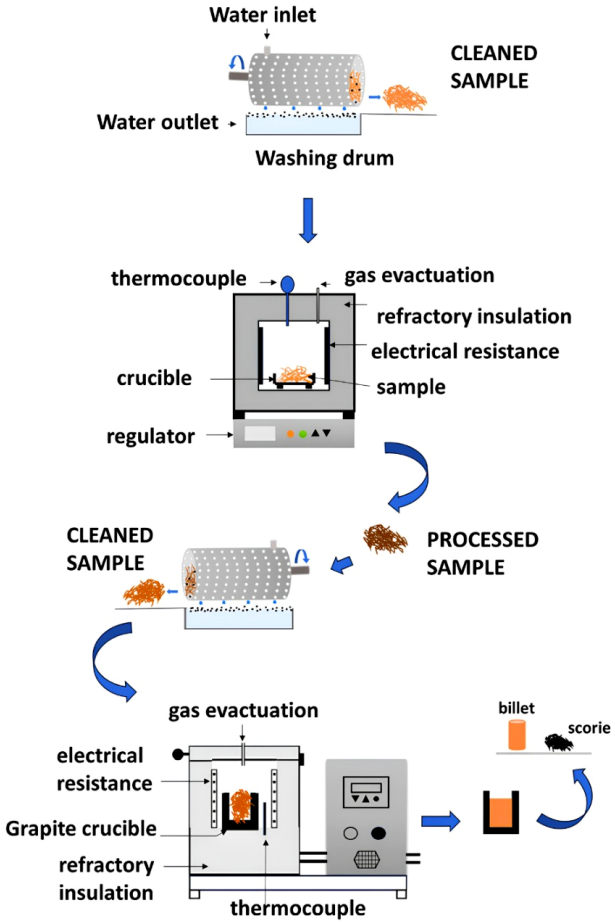

Figure 4. Stages of pretreatment and fire refining

The main objective of this pretreatment is to remove the enamel from the wires, as well as the particles that adhere to them. These particles, usually in the form of ceramics, have high melting points, which increases the recycling process's energy consumption. Additionally, enamels consist of resins and other organic compounds that can decompose and carbonise during the melting process. These residues can be incorporated into the molten metal, leading to contamination and a decrease in copper purity. The temperature of 300 °C was chosen because the melting temperatures of these enamels are below this value (polyurethane 155 – 180 °C, polyesterimide 200 °C and polyimide 240 °C) and hydrogen becomes soluble in copper above this temperature [30].

Without protective flow (i.e. a solid material placed over the melting bath to limit oxidation), the meltings were conducted in a Gold Tool Super Deluxe electric melting furnace, which is equipped with an adjustable thermostat, and its maximum temperature is 1200 °C. This furnace has a power consumption of 1100 W, a melting capacity of 2 kg, and its crucible is made from high-density graphite, in accordance with the specifications of the SIGRAFINE® R7510 grade. Every melting experiment begins by measuring the initial mass of the sample before it is placed in the crucible. Once the melting temperature is selected, the scheduling of the melting process begins. Casting begins as soon as the furnace has reached the desired temperature.

The black copper casting billets (Fig. 5) were machined on a lathe before being analysed by SPECTROMAXx optical emission spectrometer to determine their chemical composition. Calibrating this measuring instrument with a certified standard resulted in a standard deviation of 2 %. It should be noted that the chemical composition represents the average of more than four measurements taken on each billet.

Figure 5. Products obtained from separate fusions of untreated and treated samples: billet (left) and slag (right)

A Leica DM LM light optical microscope was used to reveal the microstructure of the billets, which are first polished and etched with an aqueous solution of iron (III) chloride (20 g/l). After etching, the billets were carefully rinsed with distilled water and dried to prepare them for microscopic examination.

An energy dispersive spectroscopy (EDS) analysis was performed using the JEOL JSC-IT100 scanning electron microscope (SEM) to determine the atomic composition of the individual points of these billets. After identifying the optimum temperature to achieve maximum copper purity, X-ray fluorescence (XRF) analysis was performed specifically on the treated and untreated Cliff samples slag due to their quantities compared to the negligible amount of the Berry sample slag. In addition, an X-ray diffraction (XRD) analysis was

carried out on the slag from the treated Cliff sample, which is considered to be the most relevant sample for our study.

To measure thermal conductivity, the billet cast from the melting of the treated sample at 1120 °C was cut into a disc with a diameter of 2.5 cm and a thickness of 3.34 mm. This disc was then placed between the cold and hot sections of the PA Hilton linear heat conduction unit H112A (Fig. 6). Configured as a column, this unit is equipped with eight thermocouples spaced 15 mm apart, connected to the heat transfer service unit for temperature measurement. The variation in voltage at the H112A unit allows heat flux adjustment within the column.

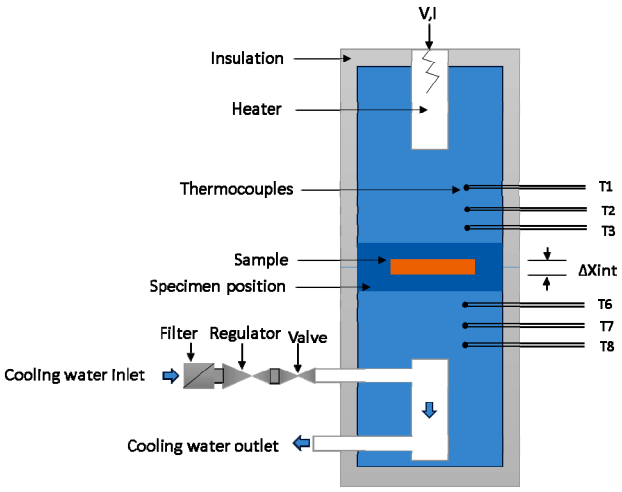

Figure 6. Components of linear heat conduction unit H112A

The calculation was according to the user manual of the linear heat conduction unit H112A, i.e.

$$\dot{Q} = UI,$$
$$T_{hot} = T_3 - \frac{T_2 - T_3}{2},\ T_{cold} = T_6 + \frac{T_6 - T_7}{2},$$
$$\Delta X = \Delta X_{int} + 0.015,$$
$$K = \frac{UI\Delta X}{A(T_{hot} - T_{cold})}, \quad (1)$$

where $\dot{Q}$ is the heat transfer rate in W, T_{hot} is the temperature on the hot side of the sample in K, T_{cold} is the temperature on the cold side of the sample in K, U is the voltage applied to the heater in V, I is the electric current through the heater in A, A is the cross-sectional area of the sample perpendicular to the heat flow direction in m^2, ΔX_{int} is the sample thickness in m and K is the thermal conductivity of a sample in W/mK.

The approximate value of the electrical conductivity was determined using the Wiedemann-Franz law [31], given by

$$\sigma = \frac{K}{L_0 T}, \quad (2)$$

where σ is the electrical conductivity in S/m, T is the temperature in K and L_0 is the Lorenz number (approximately equal to 2.23×10^{-8} WΩ/K^2).

3. Results

3.1 Copper content

The primary challenge in fire refining is casting at appropriate temperatures to measure the concentrations of copper and impurities in the baths. Although the furnace is expected to reach temperatures up to 1200 °C as per its technical specifications, difficulties arose when conducting tests at temperatures exceeding 1105 °C. This ceramic band resistance furnace does not have an efficient cooling system. After four melts, the ceramic band resistance fails at 1105 °C and cannot be repaired, requiring replacement. Consequently, more than nine resistances were used to obtain the results for each sample.

For the first (reference sample Berry), fire refining revealed that the highest copper concentration of 99.968 wt. % was obtained at 1090 °C (Fig. 7). It is important to note that the results of this refining in terms of copper content increase from 1090 to 1120 °C. After reaching a peak at this last temperature, the content decreases significantly and reaches its minimum value at 1180 °C.

For the untreated Cliff sample, the copper content follows a similar trend to that of Berry with increasing temperature (Fig. 8). Specifically, copper content reaches its maximum of 99.936 wt. % at 1120 °C. After increasing between 1090 and 1120 °C, it decreases for other temperatures.

For the treated Cliff sample, the copper content follows a similar trend to that of the previous samples (Fig. 9). After an increase to reach its maximum at 1120 °C with 99.952 wt. %, it decreases for the other temperatures. A comparison of its maximum copper content to that of the untreated Cliff sample clearly reveals an increase of 0.02 %. This observation highlights the significant impact of the mentioned pretreatment on copper purification.

3.2 Impurities content

With a minimum value of 0.032 wt. % at 1120 °C, the content of metal impurities in the casting of the Berry sample decreases between 1090 and 1120 °C (Fig. 10). Afterwards, it starts to

increase for other temperatures. With the exception of zinc, all chemical elements affecting the mechanical and electrical properties of the final product have concentrations lower than 0.01 wt. % (Table 2). Despite this, the zinc concentration decreased from 0.051 wt. % (Table 1) to values not exceeding 0.016 wt. %. It is noteworthy that the variation in the value of volatile impurities (Zn, As and P) follows the same trend as that of all impurities combined.

Regarding the impurities present in the casting of the untreated Cliff sample, the same findings as before were noticed, with a minimum content of 0.062 wt. % at 1120 °C (Fig. 11). Two things stand out according to Table 3: the zinc concentration ranges from 0.02 to 0.03 wt. %, and that of iron is

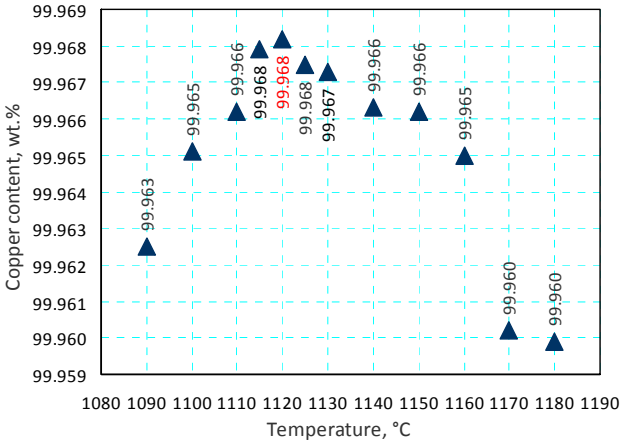

Figure 7. Variation of copper content with melting temperature for Berry sample

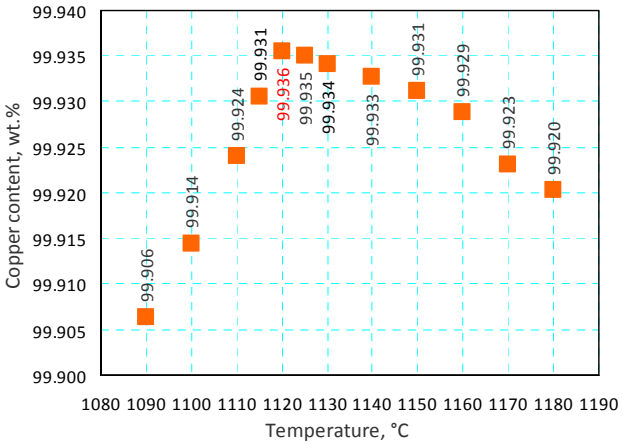

Figure 8. Variation of copper content with melting temperature for untreated Cliff sample

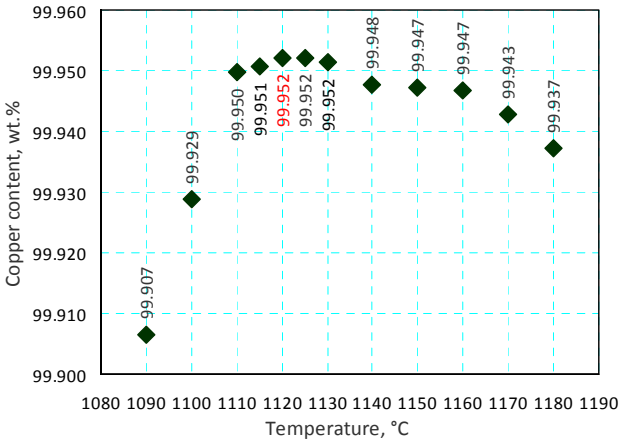

Figure 9. Variation of copper content with melting temperature for treated Cliff sample

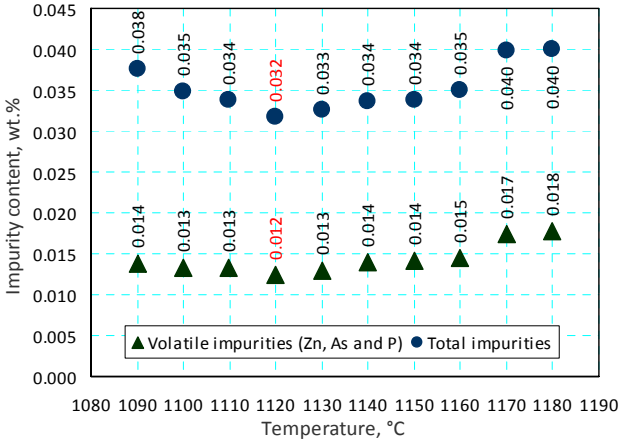

Figure 10. Variation of impurities content with melting temperature for Berry sample

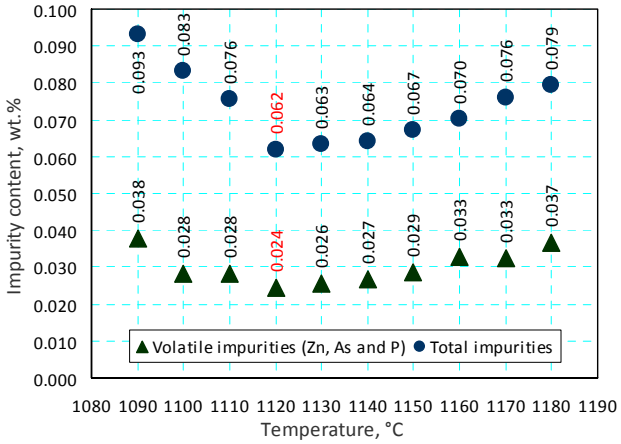

Figure 11. Variation of impurities content with melting temperature for untreated Cliff sample

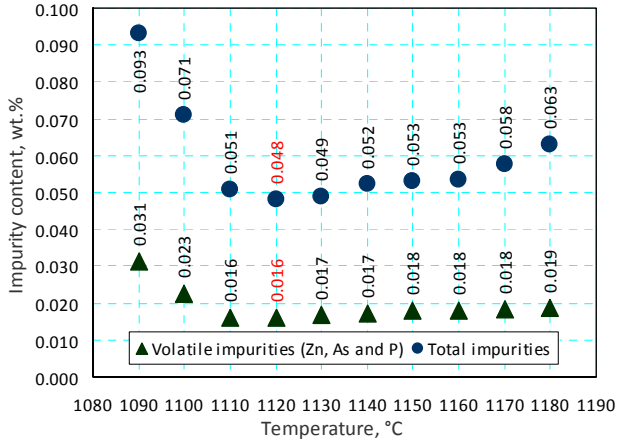

Figure 12. Variation of impurities content with melting temperature for treated Cliff sample

around 0.01 wt. %. The presence of other metallic elements remains negligible.

With a value of 0.048 wt. % at 1120 °C (Fig. 12), the impurities content in the casting of the treated Cliff sample decreased by 23 % compared to that of the same type of untreated sample at this temperature. The way this content varies with the melting temperature is similar to that previously noticed. The volatile impurities present a linear trend that converges to 0.02 wt. %. Compared to the other metallic elements, only zinc has a significant concentration that fluctuates around 0.01 wt. % (Table 4).

3.3 Thermal conductivity

In general, the thermal conductivity of metals can be expressed in the form $K = K_E + K_G$, where K_E represents the thermal conductivity due to electron conduction and K_G to phonon conduction [32]. The temperatures (Fig. 6) needed for this determination were measured experimentally under varying voltages (Table 5).

Table 2. Average chemical composition (wt. %) of Berry sample at different melting temperatures (*T*)

T, °C	1090	1100	1110	1115	1120	1125	1130	1140	1150	1160	1170	1180
Zn	0.01267	0.01226	0.01223	0.01210	0.01128	0.01159	0.01179	0.01282	0.01283	0.01330	0.01628	0.01631
Pb	0.00030	0.00030	0.00030	0.00030	0.00030	0.00030	0.00030	0.00030	0.00030	0.00030	0.00030	0.00030
Sn	0.00020	0.00020	0.00020	0.00020	0.00020	0.00020	0.00020	0.00020	0.00020	0.00020	0.00020	0.00020
Ni	0.00020	0.00020	0.00020	0.00020	0.00020	0.00020	0.00020	0.00020	0.00020	0.00020	0.00020	0.00020
As	0.00024	0.00027	0.00022	0.00024	0.00022	0.00031	0.00024	0.00024	0.00030	0.00030	0.00025	0.00049
Sb	0.00146	0.00170	0.00144	0.00151	0.00178	0.00189	0.00190	0.00189	0.00214	0.00228	0.00197	0.00228
Ag	0.00030	0.00030	0.00030	0.00044	0.00030	0.00041	0.00030	0.00030	0.00041	0.00031	0.00030	0.00030
P	0.00082	0.00081	0.00091	0.00088	0.00086	0.00082	0.00090	0.00088	0.00094	0.00095	0.00091	0.00090
Fe	0.00126	0.00136	0.00311	0.00143	0.00119	0.00121	0.00127	0.00105	0.00139	0.00184	0.00346	0.00265
Si	0.00050	0.00050	0.00050	0.00050	0.00050	0.00050	0.00050	0.00050	0.00050	0.00050	0.00080	0.00083
Al	0.00030	0.00030	0.00030	0.00030	0.00030	0.00030	0.00030	0.00030	0.00030	0.00030	0.00030	0.00030
Be	0.00010	0.00010	0.00010	0.00010	0.00010	0.00010	0.00010	0.00010	0.00010	0.00010	0.00010	0.00010
Other*	0.01918	0.01657	0.01399	0.01386	0.01456	0.01467	0.01467	0.01488	0.01422	0.01439	0.01470	0.01520
Cu	99.9625	99.9651	99.9662	99.9679	99.9682	99.9675	99.9673	99.9663	99.9662	99.9650	99.9602	99.9599

*Mn, Mg, Cr, Te, Cd, Bi, Co, S, Zr, Au, B, Ti, Se and Pt

Table 3. Average chemical composition (wt. %) of untreated Cliff sample at different melting temperatures (*T*)

T, °C	1090	1100	1110	1115	1120	1125	1130	1140	1150	1160	1170	1180
Zn	0.03626	0.02668	0.03635	0.02408	0.02288	0.02399	0.02420	0.02523	0.02717	0.03101	0.03099	0.03602
Pb	0.00030	0.00030	0.00030	0.00030	0.00030	0.00030	0.00030	0.00030	0.00030	0.00030	0.00030	0.00030
Sn	0.00075	0.00064	0.01005	0.00066	0.00256	0.00256	0.00260	0.00263	0.00269	0.00269	0.00269	0.00266
Ni	0.00027	0.000288	0.00267	0.00026	0.00020	0.00020	0.00021	0.00021	0.00022	0.00022	0.00022	0.00020
As	0.00051	0.00049	0.00053	0.00041	0.00058	0.00068	0.00057	0.00057	0.00063	0.00066	0.00061	0.00060
Sb	0.00371	0.00369	0.00327	0.00363	0.00324	0.00336	0.00335	0.00330	0.00550	0.00360	0.00329	0.00374
Ag	0.00030	0.00176	0.00141	0.00183	0.00240	0.00370	0.00290	0.00290	0.00240	0.00198	0.00210	0.00230
P	0.00094	0.00119	0.00128	0.00096	0.00098	0.00094	0.00097	0.00095	0.00098	0.00101	0.00098	0.00011
Fe	0.00400	0.00445	0.00368	0.01905	0.01175	0.01148	0.01127	0.01105	0.01136	0.01191	0.01691	0.01513
Si	0.00050	0.00124	0.00093	0.00050	0.00050	0.00050	0.00050	0.00050	0.00053	0.00050	0.00050	0.00058
Al	0.03000	0.02662	0.00030	0.00030	0.00030	0.00030	0.00030	0.00030	0.00030	0.00030	0.00030	0.00030
Be	0.00010	0.00010	0.00010	0.00010	0.00010	0.00010	0.00010	0.00010	0.00010	0.00010	0.00010	0.00010
Other*	0.01540	0.01570	0.01470	0.01520	0.01610	0.01490	0.01590	0.01600	0.01490	0.01590	0.01690	0.01720
Cu	99.9064	99.9144	99.924	99.9305	99.9355	99.9351	99.93411	99.9327	99.9311	99.9289	99.9231	99.9203

*Mn, Mg, Cr, Te, Cd, Bi, Co, S, Zr, Au, B, Ti, Se and Pt

Table 4. Average chemical composition (wt. %) of treated Cliff sample at different melting temperatures (*T*)

T, °C	1090	1100	1110	1115	1120	1125	1130	1140	1150	1160	1170	1180
Zn	0.02925	0.02066	0.01491	0.01489	0.01409	0.01483	0.01513	0.01553	0.01609	0.01617	0.01644	0.01673
Pb	0.00030	0.00030	0.00079	0.00030	0.00030	0.00030	0.00030	0.00030	0.00030	0.00030	0.00030	0.00030
Sn	0.00134	0.00025	0.00218	0.00288	0.00298	0.00195	0.00195	0.00199	0.00233	0.00197	0.00231	0.00296
Ni	0.00361	0.00357	0.00333	0.00397	0.00399	0.00393	0.00433	0.00501	0.00587	0.00556	0.00713	0.00879
As	0.00061	0.00060	0.00057	0.00054	0.0004	0.00040	0.00051	0.00059	0.00066	0.00056	0.00057	0.00068
Sb	0.00426	0.00364	0.00403	0.00304	0.00383	0.00390	0.00392	0.00403	0.00411	0.00413	0.00403	0.00485
Ag	0.00316	0.00291	0.00331	0.00231	0.00234	0.00287	0.00291	0.00311	0.00325	0.00347	0.00366	0.00398
P	0.00141	0.00134	0.00058	0.00159	0.00145	0.00144	0.00131	0.00098	0.00111	0.00132	0.00129	0.00144
Fe	0.00243	0.00470	0.00400	0.00374	0.00287	0.00200	0.00210	0.00227	0.00299	0.00317	0.00377	0.00397
Si	0.00050	0.00590	0.00050	0.00050	0.0005	0.00050	0.00050	0.00050	0.00050	0.00050	0.00080	0.00083
Al	0.03310	0.01010	0.00030	0.00030	0.0003	0.00030	0.00030	0.00030	0.00030	0.00030	0.00030	0.00030
Be	0.00010	0.00010	0.00010	0.00010	0.0001	0.00010	0.00010	0.00010	0.00010	0.00010	0.00010	0.00010
Other*	0.01320	0.01710	0.01610	0.01500	0.0151	0.01570	0.01560	0.01770	0.01550	0.01590	0.01680	0.01800
Cu	99.9066	99.9288	99.9498	99.9508	99.9522	99.952	99.9515	99.9476	99.9473	99.9468	99.9429	99.9373

*Mn, Mg, Cr, Te, Cd, Bi, Co, S, Zr, Au, B, Ti, Se and Pt

Table 5. Experimental values for billet cast from treated Cliff sample melting

U, V	54	82	109	106	107	122
I, A	0.54	0.80	1.12	1.10	1.11	1.27
T_1, °C	26.3	36.0	48.8	48.7	49.2	55.3
T_2, °C	25.5	34.2	45.7	45.6	46.2	51.6
T_3, °C	24.6	32.3	42.6	42.5	43.0	47.8
T_6, °C	20.4	23.1	26.5	26.5	26.7	28.3
T_7, °C	19.7	21.5	23.8	23.7	23.9	25.0
T_8, °C	19.0	20.0	21.1	21.1	21.2	21.6

According to Table 6, the average thermal conductivity of this treated Cliff sample can be estimated at 338 W/mK. This value is consistent with those mentioned in the study [33] and close to pure copper of 380 W/mK.

4. Discussion

4.1 Variations in copper and impurities content

In order to understand the optimal results obtained at 1120 °C, as well as the opposite variations in the copper (Figs. 7, 8 and 9) and impurities content (Figs. 10, 11 and 12) as a function of the melting temperature, the XRF analyses were performed on melt slag of treated and untreated Clift samples at this temperature. The results of these analyses revealed the presence of copper in these slags with appreciable quantities of 32.15 wt. % for treated and 56.62 wt. % for untreated Cliff samples (Table 7), as well as other impurities in the form of oxides. Consequently, for temperatures lower than 1120 °C, the increase in the copper content and the reduction in impurities content are justified by the volatilisation of impurities (Zn, As and P) whose vapour pressures are higher than that of copper [34], as well as by the oxidation of other impurities. For temperatures higher than 1120 °C,

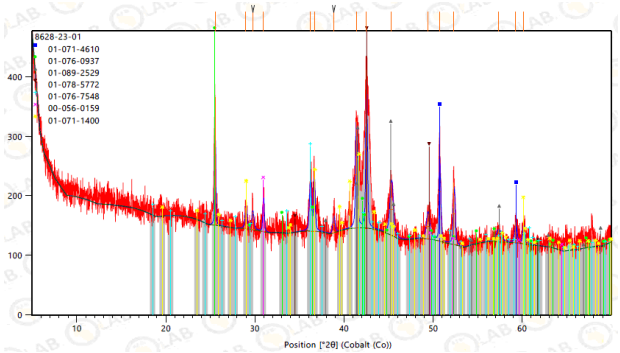

Peak code	Compound chemical formula
01-071-4610	Cu
01-076-0937	SiO_2
01-089-2529	CuO
01-078-5772	Cu_2O
01-076-7548	$Ca_2Mg(Si_2O_7)$
00-056-0159	C
01-071-1400	Fe_2SiO_4

Figure 13. Results of the XRD analysis of the treated Clift sample slag

Table 6. Thermal conductivity for billet cast from treated sample melting

ΔX, m	A, m^2	$\dot{Q}$, W	T_{hot}, K	T_{cold}, K	ΔT, K	$\Delta T/\Delta X$, K/m	K, W/mK
1.83×10^{-2}	4.91×10^{-4}	29.2	297.2	293.8	3.4	185.4	320.6
1.83×10^{-2}	4.91×10^{-4}	65.6	304.4	296.9	7.4	406.2	329.2
1.83×10^{-2}	4.91×10^{-4}	122.1	314.1	300.9	13.2	719.7	345.7
1.83×10^{-2}	4.91×10^{-4}	116.6	314.0	300.9	13.1	711.6	334.0
1.83×10^{-2}	4.91×10^{-4}	118.8	314.4	301.1	13.3	725.2	333.8
1.83×10^{-2}	4.91×10^{-4}	154.9	318.9	303.0	15.9	869.7	363.1

Table 7. Results of the XRF analysis

Untreated Cliff sample																				
Compound	Al_2O_3	CaO	Fe_2O_3	K_2O	MgO	MnO	P_2O_5	S	SiO_2	TIO_2	Cu									
wt. %	6.95	5.72	1.20	0.25	1.19	0.01	1.81	1.92	2.72	1.22	56.62									
Untreated Cliff sample																				
Element	As	B	Ba	Be	Bi	Cd	Co	Cr	Ge	Li	Mo	Ni	Pb	Sb	Se	Sn	Sr	Ta	Ti	Y	Zn
ppm	32	47	187	< 1	< 10	< 1	< 5	164	< 10	< 20	20	87	124	188	< 30	142	231	41	< 1	4	1022
Treated Cliff sample																				
Compound	Al_2O_3	CaO	Fe_2O_3	K_2O	MgO	MnO	P_2O_5	S	SiO_2	TiO_2	Cu	Zn								
wt. %	13.08	5.77	31.17	0.56	1.26	1.54	1.89	0.01	14.84	0.65	32.15	3.17								

the copper in the slag increases with temperature in the form of oxide. Therefore, it's content in the billet decreases as that of impurities increases. To confirm this, additional XRD analysis of the treated Clift sample slag clearly revealed the presence of copper and some impurities in the form of oxides (Fig. 13).

4.2 Zinc presence

The variation of the zinc concentration as a function of the melting temperature follows a trend similar to that noticed for the copper and impurities contents. This element stands out from other impurities by its significant presence in the compositions of the three cast billets (Fig. 14). By disregarding any uneven distribution of impurities within these billets, considering that over four measurements were taken at different locations. The high zinc concentration can be attributed to its solubility in the solid phase and complex chemical reactions involving precipitation or the formation of intermetallic phases (Fig. 15) [35,36]. The difference in reflectivity observed in the macrostructure of both treated and untreated billets cast at 1120 °C, visible through distinct colour contrasts (Fig. 16), suggests the presence of different phases or compositional variations.

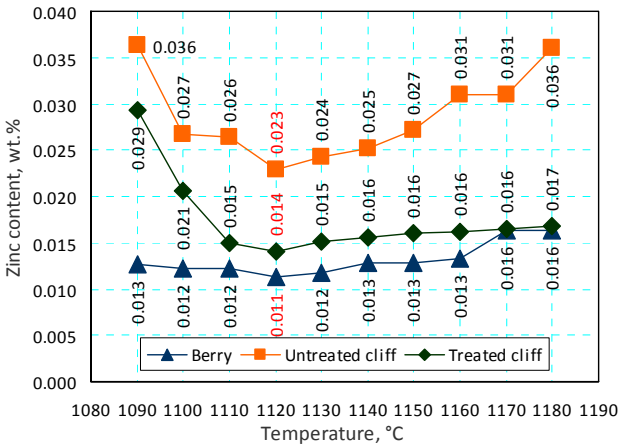

Figure 14. Variation of zinc content in billets as a function of melting temperature for the three copper scrap samples

4.3 Validation of content variations

To confirm the copper and impurities content values found at 1120 °C for all samples, the vicinity of this temperature was explored by two additional fusions with a difference of 5 °C, namely at 1115 and 1125 °C. The results shown in Figure 17 clearly confirm that the copper and impurities values at 1120 °C represent the maximum copper concentration and the minimum impurities concentration for all samples.

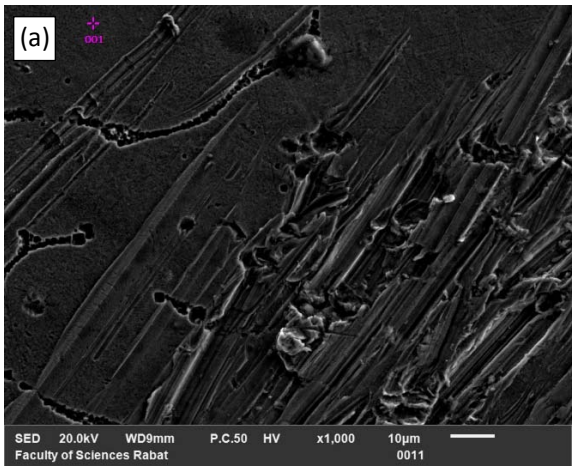

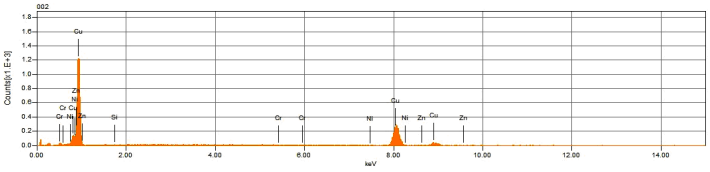

Element	Si	Cr	Ni	Zn	Cu
wt. %	0.48	0.30	0.39	1.09	97.75

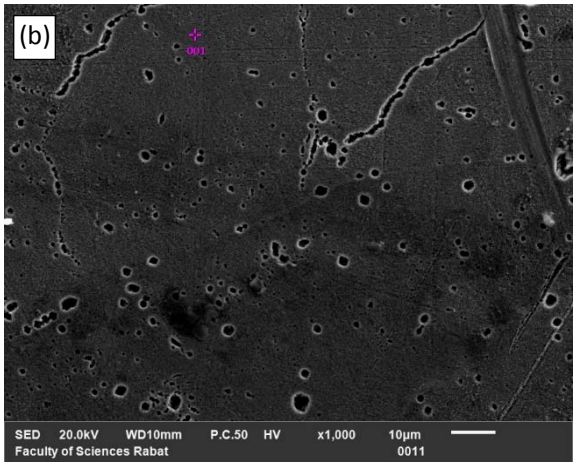

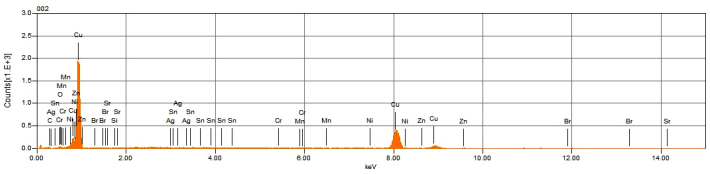

Element	Si	Cr	Mn	Ni	Zn	Br	Sr	Ag	Sn	Cu
wt. %	0.48	0.09	0.05	0.02	1.11	0.09	0.56	0.66	0.36	96.39

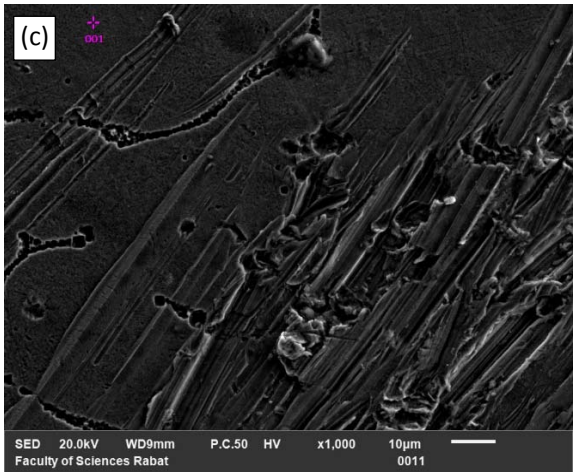

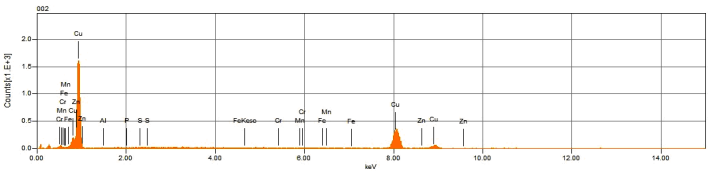

Element	Al	P	S	Cr	Mn	Fe	Zn	Cu
wt. %	0.22	0.13	0.20	0.22	0.31	0.44	1.04	97.44

Figure 15. SEM micrographs and EDS point analyses of billets cast at 1120 °C from different copper scrap samples: (a) Berry, (b) untreated Cliff and (c) treated Cliff

Figure 16. Macrostructures (50 ×) of billets cast at 1120 °C from different copper scrap samples: (a) Berry, (b) untreated Cliff and (c) treated Cliff

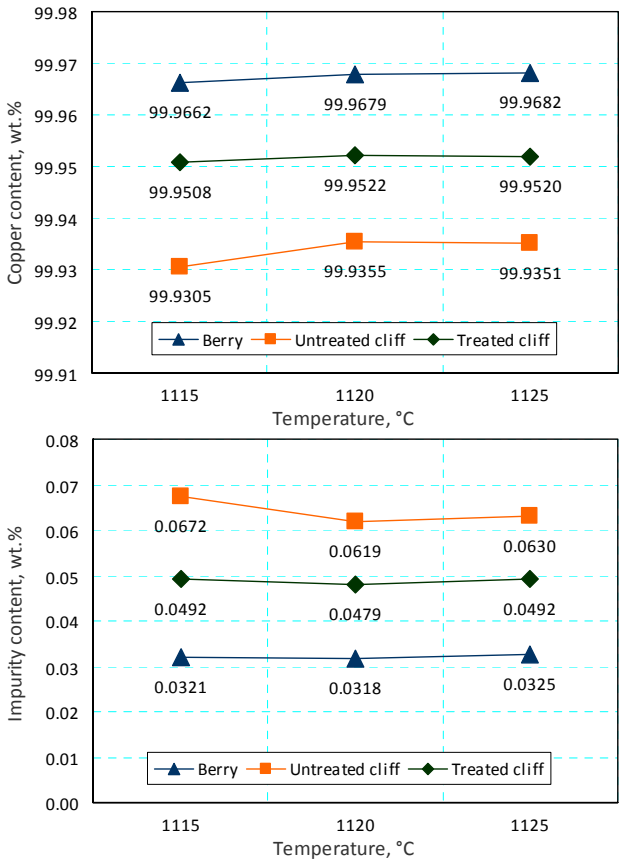

Figure 17. Evolution of copper and impurity contents as a function of melting temperature in the vicinity of 1120 °C

4.4 Electrical conductivity

The electrical conductivity is calculated using Equation (2), substituting the known values and using the thermal conductivity value K = 338 W/mK determined in section 3.3.

$$\sigma = \frac{338}{2.23\times10^{-8}(20+273)} = 5.17\times10^{7}\ 1/\Omega m \quad (3)$$

This corresponds to approximately 88 % IACS (International Annealed Copper Standard) according to

$$\%IACS = \left(\frac{\sigma_{measured}}{\sigma_{copper}}\right)100, \quad (4)$$

where $\sigma_{copper} = 5.85 \times 10^7$ 1/Ωm.

These values found for thermal and electrical conductivities are significantly close to those of pure copper, namely 380 W/mK for thermal conductivity and 58.5×10^6 1/Ωm for electrical conductivity. Given these properties, the material demonstrates considerable potential for industrial applications. It is particularly well-suited for water-cooled tuyeres, which necessitate a minimum electrical conductivity of 86 % IACS [37].

5. Conclusions

To determine the optimal casting temperature, a fire refining process was conducted on three samples of the copper scrap at varying temperatures ranging from 1090 to 1180 °C. This temperature was recorded at 1120 °C, where the copper concentration is at its highest level while the impurity concentration is at its lowest. This result was confirmed by melting samples at temperatures near 1120 °C, specifically at 1115 and 1125 °C.

The pretreatment included water washing in a rotary drum, air drying and heating at 300 °C to remove enamels that had a significant impact on the copper and impurity concentration. Compared to the untreated sample, this process increased copper concentration by 0.02 % and reduced impurity concentration by 23 % in the treated sample. With only a slight difference in copper concentration (decrease of 0.02 %), this method achieved copper concentration very close to that of the reference Berry sample.

Considering the values found for purity, thermal conductivity (338 W/mK) and electrical conductivity (88 % IACS), which meet the requirements of certain standards such as ASTM B171/B171M and ASTM B249/B249M, black copper produced from scrap subjected to this pretreatment process can serve as raw material for specific industries. These industries include industrial boiler-making (tanks, heat exchangers, pipes, tubes, evaporators, coils, etc.) and the manufacturing of copper strips for electrical purposes.

Acknowledgement

We would like to express our gratitude to everyone at the BMC and CNRST for their invaluable support throughout this research. A special thanks goes to professors Hamid Mounir and Yassine Zalim for their unwavering support. We also wish a speedy recovery to Professor Bachir Hamri.

References

[1] M.G. Ali, Copper Production in the Next 50 Years – The Main Trends, Process & Furnace Developments, Scrap as Raw-Materials, Waste Management, and Copper Recovery, MSc thesis, Aalto University, Espoo, 2023.

[2] M. Ruhrberg, Assessing the recycling efficiency of copper from end-of-life products in Western Europe, Resources, Conservation and Recycling,

Vol. 48, No. 2, 2006, pp. 141-165, DOI: 10.1016/j.resconrec.2006.01.003
[3] L. Ciacci, T. Fishman, A. Elshkaki, T.E. Graedel, I. Vassura, F. Passarini, Exploring future copper demand, recycling and associated greenhouse gas emissions in the EU-28, Global Environmental Change, Vol. 63, 2020, Paper 102093, DOI: 10.1016/j.gloenvcha.2020.102093
[4] The World Copper Factbook 2020, International Copper Study Group, Lisbon, 2020.
[5] J. Li, D. Eheliyagoda, Y. Geng, Z. Yang, X. Zeng, Examining the influence of copper recycling on prospective resource supply and carbon emission reduction, Fundamental Research, Vol. 5, No. 2, 2025, pp. 740-747, DOI: 10.1016/j.fmre.2022.09.022
[6] Y. Sugimura, T. Kawasaki, S. Murakami, Potential for increased use of secondary raw materials in the copper industry as a countermeasure against climate change in Japan, Sustainable Production and Consumption, Vol. 35, 2023, pp. 275-286, DOI: 10.1016/j.spc.2022.11.007
[7] W.D. Riley, H.V. Makar, Impurity effects in secondary copper alloys, Conservation & Recycling, Vol. 9, No. 4, 1986, pp. 315-323, DOI: 10.1016/0361-3658(86)90066-4
[8] S. Xiao, W. Xiong, L. Wang, Q. Ren, The treatment technology of recycling scrap wire and cable, in Proceedings of the 2015 4th International Conference on Sustainable Energy and Environmental Engineering (ICSEEE 2015), 20-21.12.2015, Shenzhen, China, pp. 500-503, DOI: 10.2991/icseee-15.2016.82
[9] A. Loibl, L.A. Tercero Espinoza, Current challenges in copper recycling: Aligning insights from material flow analysis with technological research developments and industry issues in Europe and North America, Resources, Conservation and Recycling, Vol. 169, 2021, Paper 105462, DOI: 10.1016/j.resconrec.2021.105462
[10] J. Cui, E. Forssberg, Mechanical recycling of waste electric and electronic equipment: A review, Journal of Hazardous Materials, Vol. 99, No. 3, 2003, pp. 243-263, DOI: 10.1016/S0304-3894(03)00061-X
[11] M.E. Schlesinger, M.J. King, K.C. Sole, W.G. Davenport, Collection and processing of recycled copper, in Extractive Metallurgy of Copper, Elsevier, Amsterdam, 2011, pp. 373-387, DOI: 10.1016/B978-0-08-096789-9.10018-6
[12] D. Davies, Secondary copper recovery, Resources Policy, Vol. 1, No. 5, 1975, pp. 246-252, DOI: 10.1016/0301-4207(75)90051-3
[13] M. Bonnin, C. Azzaro-Pantel, L. Montastruc, L. Pibouleau, S. Domenech, J. Villeneuve, Development of a sustainable copper scrap management model, Computer Aided Chemical Engineering, Vol. 32, 2013, pp. 613-618, DOI: 10.1016/B978-0-444-63234-0.50103-2
[14] A.W. Fletcher, Review lecture: Metal recycling from scrap and waste materials, Proceedings of the Royal Society of London A, Vol. 351, No. 1665, 1976, pp. 151-178, DOI: 10.1098/rspa.1976.0135
[15] N.K. Dosmukhamedov, E.E. Zholdasbay, G.B. Nurlan, Ultra-pure Cu obtaining using zone melting: influence of liquid zone width on impurities' behavior, Non-ferrous Metals, Vol. 43, No. 2, 2017, pp. 15-20, DOI: 10.17580/nfm.2017.02.03
[16] S. Rzadkosz, M. Kranc, A. Garbacz-Klempka, J. Kozana, M. Piękoś, *Refining processes in the copper casting technology*, Metalurgija, Vol. 54, No. 1, 2015, pp. 259-262.
[17] M. Mominul Haque, H. Kim, M.-S. Kong, H.-S. Hong, K.-S. Kim, C.S. Lee, Recycling copper from waste copper wire using an applied voltage, International Journal of Precision Engineering and Manufacturing, Vol. 13, No. 7, 2012, pp. 1251-1254, DOI: 10.1007/s12541-012-0167-3
[18] N.K. Dosmukhamedov, E.E. Zholdasbay, G.B. Nurlan, M.B. Kurmanseitov, Employment of zone melting to obtain ultrapure copper: Behavioural patterns of impurity metals, Цветные металлы, No. 7, 2017, pp. 34-41, DOI: 10.17580/tsm.2017.07.06
[19] K. Vutova, V. Stefanova, V. Vassileva, M. Kadiyski, Behaviour of impurities during electron beam melting of copper technogenic material, Materials, Vol. 15, No. 3, 2022, Paper 936, DOI: 10.3390/ma15030936
[20] A. Smalcerz, L. Blacha, Removal of lead from blister copper by melting in the induction vacuum furnace, Archives of Foundry Engineering, Vol. 20, No. 2, 2020, pp. 84-88, DOI: 10.24425/afe.2020.131307
[21] A. Smalcerz, L. Blacha, Vacuum refinning cooper blister to remove antimony, Metalurgija, Vol. 59, No. 3, 2020, pp. 358-360.
[22] M.E. Schlesinger, M.J. King, K.C. Sole, W.G. Davenport, Electrolytic refining, in Extractive Metallurgy of Copper, Elsevier, Amsterdam, 2011, pp. 251-280, DOI: 10.1016/B978-0-08-096789-9.10014-9
[23] V.G. Lisienko, S.I. Holod, V.P. Zhukov, Modeling of metallurgical process of copper fire refining, in VII All-Russian Scientific and Practical Conference of Students, Graduate Students and Young Scientists (TIM'2018), Knowledge E, Dubai, 2018, pp. 241-250, DOI: 10.18502/keg.v3i5.2676
[24] Y. Fu, J. Chen, N. Liu, Y. Lu, T. Li, G. Yin, Study of ultrahigh-purity copper billets refined by vacuum melting and directional solidification,

Rare Metals, Vol. 30, No. 3, 2011, pp. 304-309, DOI: 10.1007/s12598-011-0388-0

[25] Y.-O. Yoon, H.-H. Jo, H. Cho, S.K. Kim, Y.-J. Kim, Effect of distribution coefficient on copper purification by zone refining process, Materials Science Forum, Vol. 449-452, 2004, pp. 173-176, DOI: 10.4028/www.scientific.net/MSF.449-452.173

[26] D. Wang, L. Wang, H. Yu, Y. Tian, B. Yang, B. Xu, D. Liang, T. Ma, Preparation of high-purity copper through vacuum distillation, Vacuum, Vol. 218, 2023, Paper 112566, DOI: 10.1016/j.vacuum.2023.112566

[27] J.Y. Choi, D.S. Kim, Production of ultrahigh purity copper using waste copper nitrate solution, Journal of Hazardous Materials, Vol. 99, No. 2, 2003, pp. 147-158, DOI: 10.1016/S0304-3894(02)00312-6

[28] D.W. Green, M.Z. Southard (Ed.), Perry's Chemical Engineers' Handbook, McGraw-Hill Education, New York, 2019.

[29] Scrap Specifications Circular, Institute of Scrap Recycling Industries, Washington, 2022.

[30] A. Morillo, J. Moisan, F. Santini, J. Hérenguel, Traitements de dégazage en fonderie de métaux cuivreux (oxydation, réduction, fluosels) [Degassing treatments in copper-based alloy foundry (oxidation, reduction, fluoride fluxes)], Revue de Métallurgie, Vol. 65, No. 2, 1968, pp. 145-149, DOI: 10.1051/metal/196865020145 [in French].

[31] Z. Wang, Q. Li, J. Ren, J. Chen, Y. Zhang, H. Chen, H. Liu, Prediction of electrical/thermal conductivity in as-cast Mg binary alloys, Journal of Materials Research and Technology, Vol. 27, 2023, pp. 5924-5934, DOI: 10.1016/j.jmrt.2023.10.243

[32] J. Tuttle, E. Canavan, M. DiPirro, Thermal and electrical conductivity measurements of CDA 510 phosphor bronze, AIP Conference Proceedings, Vol. 1219, No. 1, 2010, pp. 55-62, DOI: 10.1063/1.3402333

[33] M.C.I. Siu, W.L. Carroll, T.W. Watson, Thermal Conductivity and Electrical Resistivity of Six Copper-Base Alloys, National Institute of Standards and Technology, Gaithersburg, 1976, DOI: 10.6028/NBS.IR.76-1003

[34] A. Yazawa, T. Azakami, Thermodynamics of removing impurities during copper smelting, Canadian Metallurgical Quarterly, Vol. 8, No. 3, 1969, pp. 257-261, DOI: 10.1179/cmq.1969.8.3.257

[35] K. Hanusch, H. Bussmann, Behaviour and removal of associated metals in the secondary metallurgy of copper, in Proceedings of the 3rd International Symposium on Recycling of Materials and Engineered Materials, 12-16.11.1995, Point Clear, USA, pp. 171-188.

[36] G.F. Vander Voort, Color metallography, in ASM Handbook Volume 9, Metallography and Microstructures, ASM International, Materials Park, 2004, pp. 493-512, DOI: 10.31399/asm.hb.v09.a0003752

[37] J.R. Brown, Copper and copper alloy castings, in Foseco Non-Ferrous Foundryman's Handbook, Butterworth-Heinemann, Oxford, 1999, pp. 225-251, DOI: 10.1016/B978-075064286-6/50017-6